Vol 14 No 7, July 2005
1009-1963/2005/14(07)/1334-08

Chinese Physics

© 2005 Chin. Phys. Soc.
and IOP Publishing Ltd

The crisis induced by the property transition of a system*

Dai Jun(戴 俊), Wang Wen-Xiu(王文秀), Jiang Yu-Mei(姜玉梅),
He Yue(何 阅), Chen Wen(陈 文), and He Da-Ren(何大韧)†

College of Physics Science and Technology, Yangzhou University, Yangzhou 225002, China

(Received 3 November 2004; revised manuscript received 23 March 2005)

A simultaneous transition in the property of a system from everywhere smooth and conservative to piecewise smooth and quasi-dissipative is observed in a kicked billiard when adjusting a single controlling parameter. The transition induces a special kind of crisis, which signifies a sudden change of a typical conservative stochastic web into a transient web formed by the forward image set of the discontinuity borderline of the system function. Iterations on the transient web finally fall in an escaping hole composed of an elliptic island chain, which appears right after the threshold of the property transition. The size of the hole becomes larger as the controlling parameter increases so that the iterations escape faster. The averaged lifetime of the iterations in the transient web therefore follows a power-law with a special scaling exponent. At the same time, a fat fractal forbidden web, which appears also at the threshold, grows up and cuts off more and more parts from the original conservative stochastic web so that the remnant transient web becomes thinner and thinner. We numerically show that another power law can also describe this.

Keywords: kicked billiard, crisis, stochastic web, fat fractal
PACC: 0545

1. Introduction

Piecewise smooth systems, which show frequent sudden changes, exist widely in nature. As examples can be mentioned the following: a second-order digital filter with saturation arithmetic,[1−3] relay control systems (power converters, AC and DC electric drives, adaptive control systems, etc.), [4−6] pulse-width modulated systems,[1] mechanical systems with impacts or dry friction, elasto-plastic systems and so on.[7−10] Recently, piecewise smooth conservative maps attract the attention of scientific communities. Wang and Ding and colleagues studied an electronic relaxation oscillator with over-voltage protection.[11−13] Jiang *et al*[14] studied a kicked rotor fallen in a piecewise smooth potential. We notice that, in such systems, one may observe a transition of the property of the system from everywhere smooth and conservative to piecewise smooth and quasi-dissipative when adjusting a single controlling parameter. The term "quasi-dissipative" property denotes a kind of weak dissipation, which leads to a linear collapse of the phase space instead of the exponential collapse of the phase space in conventional dissipative systems[14] (this will be further explained in next section). This kind of dissipation may also induce a sudden topological change (crisis) of a chaotic attractor, however the crisis shows some new characteristics. This paper reports such a crisis observed in a kicked billiard. In Section 2 we shall briefly introduce the system. In Section 3 we shall discuss the crisis and the power-law dependence of the iteration lifetime on the control parameter. In Section 4 we discuss the fat fractal forbidden web induced by the appearance of the system function's discontinuity. In Section 5 further discussion will be presented.

2. System

Physics related to the dynamics of a bouncing ball has started to be relevant since Fermi proposed that cosmic radiation originates from charged particles accelerated by moving magnetic field structures. In order to verify this idea, Ulam [15] examined the problem of a ball moving between a rigid wall and a vibrating

*Project supported by the National Natural Science Foundation of China (Grant No 10275053).
†E-mail: drhe@yzu.edu.cn

plate without dissipation. During the recent several decades the model of bouncing ball has been considered as an important theoretical model for the studies of classical and quantum chaos. In addition to that, recently scientists have realized that the model has technological importance. For example, during the last decade, great attention was devoted to mechanical alloying or high-energy ball milling—technological processes for making ultrafine amorphous or nanostructured powders. The mechanisms involved in such processes are closely related to the dynamics of the bouncing ball.[16] Also, the laser dynamics of high-performance dielectric micro-cavities is very similar to the dynamics of billiard models.[17] In these practical problems the possibilities, that particles obtain energies from environment or are kicked by a potential field, are often concerned. For this reason we consider a classical particle moving without friction inside a unit circle with an ideal rigid round wall. Each time when it collides with the wall, it is subjected to an impulsive force $F = K\sin(\theta - \alpha)$ along the tangential direction as shown in Fig.1. Here θ denotes the angular position of the particle and both K and α are constants. It is obvious that the radial velocity does not change after the kicking. We suppose that a controlling device can maintain a constant particle's radial velocity v_0 when it moves in the upper semicircle, while the device keeps the radial velocity as $v_0 - \beta$ when it is in the lower semicircle. By calculating the change of the momentum of the moving particle from just before the nth kick to just before the $(n+1)$th kick, one obtains

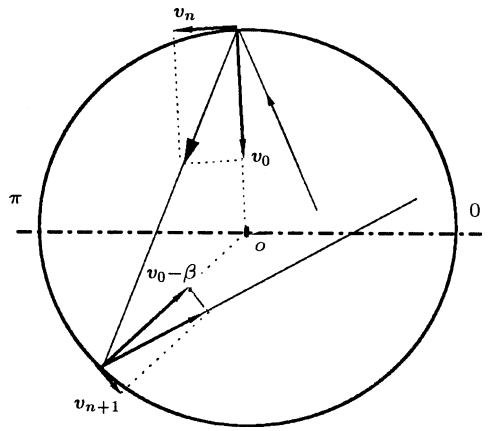


Fig.1. A schematic to show the kicked billiard.

$$f_1 : \begin{cases} v_{n+1} = v_n + K\sin(\theta_n - \alpha) \\ \theta_{n+1} = \theta_n + \pi - 2\mathrm{arctg}(v_{n+1}/v_0) \end{cases} \quad \theta_n \in [0, \pi]\,, \tag{1}$$

$$f_2 : \begin{cases} v_{n+1} = v_n + K\sin(\theta_n - \alpha) \\ \theta_{n+1} = \theta_n + \pi - 2\mathrm{arctg}(v_{n+1}/(v_0 - \beta)) \end{cases} \quad \theta_n \in (\pi, 2\pi)\,, \tag{2}$$

where v_n denotes the particle's velocity along the tangential direction and θ_n denotes the angular position of the particle just before the nth kick. The Jacobian determinant of Eqs.(1) and (2) can be written as

$$\det J = \begin{vmatrix} \dfrac{\partial v_{n+1}}{\partial v_n} & \dfrac{\partial v_{n+1}}{\partial \theta_n} \\ \dfrac{\partial \theta_{n+1}}{\partial v_{n+1}} \times \dfrac{\partial v_{n+1}}{\partial v_n} & 1 + \dfrac{\partial \theta_{n+1}}{\partial v_{n+1}} \times \dfrac{\partial v_{n+1}}{\partial \theta_n} \end{vmatrix} = \frac{\partial v_{n+1}}{\partial v_n} = 1,$$

therefore, they are area-preserving. When β=0, Eqs.(1) and (2) are exactly the same, the system is everywhere-smooth and conservative; when $\beta \neq 0$, the system becomes piecewise continuous, the inverse maps of Eqs.(1) and (2) can be obtained as

$$\begin{cases} \theta_n = \theta_{n+1} + 2\mathrm{arctg}(v_{n+1}/v_0) - \pi \\ v_n = v_{n+1} - K\sin(\theta_n - \alpha) \end{cases} \quad \theta_n \in [0, \pi]\,, \tag{3}$$

$$\begin{cases} \theta_n = \theta_{n+1} + 2\mathrm{arctg}(v_{n+1}/(v_0 - \beta)) - \pi \\ v_n = v_{n+1} - K\sin(\theta_n - \alpha) \end{cases} \quad \theta_n \in (\pi, 2\pi)\,. \tag{4}$$

Note that in order to find an inverse image, (θ_n, v_n), the principle for selecting Eq.(3) or (4) depends on the position θ_n instead of θ_{n+1}. It leads to the possibility of finding two (θ_n, v_n) points for the same (θ_{n+1}, v_{n+1}) according to the different inverse mapping form. One may find that two phase points merge into one in some conditions. This is the so-called "noninvertibility induced by discontinuity", which is the source of the quasi-dissipative property.

When $\beta = 0$, the fixed-point solutions of maps (1) and (2), (v_n^*, θ_n^*), satisfy

$$\begin{cases} v_{n+1} = v_n^* + K\sin(\theta_n^* - \alpha) = v_n^*, \\ \theta_{n+1} = \theta_n^* + \pi - 2\mathrm{arctg}\left(\dfrac{v_{n+1}}{v_0}\right) = \theta_n^*. \end{cases}$$

The fixed point does not exist when $K \neq 0$. The period-2 orbits of maps (1) and (2), (v_n^*, θ_n^*), $(v_{n+1}^*, \theta_{n+1}^*)$, satisfy

$$\begin{cases} v_{n+1}^* = v_n^* + K\sin(\theta_n^* - \alpha), \\ \theta_{n+1}^* = \theta_n^* + \pi - 2\mathrm{arctg}\left(\dfrac{v_{n+1}^*}{v_0}\right), \end{cases}$$

$$\begin{cases} v_{n+2} = v_{n+1} + K\sin(\theta_{n+1} - \alpha) = v_n^*, \\ \theta_{n+2} = \theta_{n+1} + \pi - 2\mathrm{arctg}\left(\dfrac{v_{n+2}}{v_0}\right) = \theta_n^*. \end{cases}$$

We obtain

$$\begin{cases} v_n^* = 0, \\ \theta_n^* = \alpha + K\pi, \end{cases} \quad \begin{cases} v_{n+1}^* = 0, \\ \theta_{n+1}^* = \alpha + \pi + K\pi. \end{cases}$$

They are stable in the range $0 < K < 5$.

Similarly, we know that the fixed points do not exist when $\beta \neq 0$ and $K \neq 0$. In this case, one has to discuss the period-2 orbits under different situations. In current study we are interested only in the case when one periodic point, (v_n^*, θ_n^*), is located at $\theta_n \in [0, \pi]$, and another, $(v_{n+1}^*, \theta_{n+1}^*)$, is located at $\theta_n \in (\pi, 2\pi)$ (the orbit can be addressed as an "orbit crossing border"), the solution satisfies

$$\begin{cases} v_{n+1}^* = v_n^* + K\sin(\theta_n^* - \alpha), \\ \theta_{n+1}^* = \theta_n^* + \pi - 2\mathrm{arctg}\left(\dfrac{v_{n+1}^*}{v_0}\right), \end{cases}$$

$$\begin{cases} v_{n+2} = v_{n+1}^* + K\sin(\theta_{n+1}^* - \alpha) = v_n^*, \\ \theta_{n+2} = \theta_{n+1}^* + \pi - 2\mathrm{arctg}\left(\dfrac{v_{n+2}^*}{v_0 - \beta}\right) = \theta_n^*. \end{cases}$$

They are stable in the range $-2 < 2 - \dfrac{0.8K^2}{5-\beta} < 0$. In this article, we only discuss the situation where the parameters are fixed at $K = 4.65$, $\alpha = 1$, $v_0 = 5$. β is selected as the control parameter. It is easy to deduce that the orbit crossing border is stable when $\beta < 0.6755$. For the four-fold iteration periodic orbit, which will be discussed in this paper, one of the four periodic points, $(v_n^*, \theta_n^*) \in [0, \pi]$, should satisfy $f_2\{f_2\{f_1[f_1(v_n^*, \theta_n^*)]\}\} = (v_n^*, \theta_n^*)$. Numerically we obtain that its stability condition is $\beta < 0.5986$.

3. Stochastic web crisis

Figure 2 was drawn by evenly selecting 100 initial points in the range $\theta \in [0, 2\pi]$, $v \in [-1, 1]$, ignoring the first 50000 iterations and recording next 600 ones as $\beta = 0$. The range $v \in [-1, 1]$ is taken only for obtaining suitable figure scope. The figure will be exactly the same if we record the first 600 iterations instead since the system now is conservative and everywhere smooth. The figure shows a stochastic web and some elliptic islands. As is well known, the web should be composed of the stochastic layers along the separatrices of some hyperbolic periodic orbits and is a fat fractal.[18] One can see many evenly distributed points inside the web, which has no internal structures.

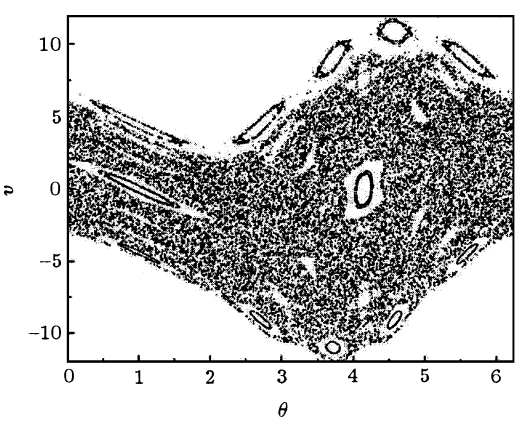


Fig.2. The phase plane at $K = 4.65$, $\alpha = 1$, $v_0 = 5$ and β=0.

Figure 3 is drawn by evenly selecting 1000 initial points in the discontinuous borderline $\{(\theta, v)|_{\theta=\pi, v\in[-1,1]}\}$ and recording the first 100 ones as $\beta = 0.01$. It should show approximately the set of the forward images of the discontinuous borderline. Mira[19] has analytically proved that in certain kinds of two-dimensional piecewise continuous noninvertible maps, like the system to be discussed in this article, the chaotic area is bounded by segments of images of the discontinuous borderlines. The numerical results shown in Fig.3 are in agreement with the conclusion in Ref.[19] and indicating that the iterations in this

stochastic web formed by the image set of the discontinuous borderline perform a chaotic motion at least in transients when $\beta \neq 0$. One should note that the web takes a very similar form to the conservative one shown in Fig.2; however a lot of thin void lines appear inside it so that the web now seems to have a kind of internal structure. We shall show in next section that the void lines form a fat fractal forbidden web, it cuts off a fat fractal part of the original conservative web, the remnant is just the stochastic web formed by the image set of the discontinuous borderlines.

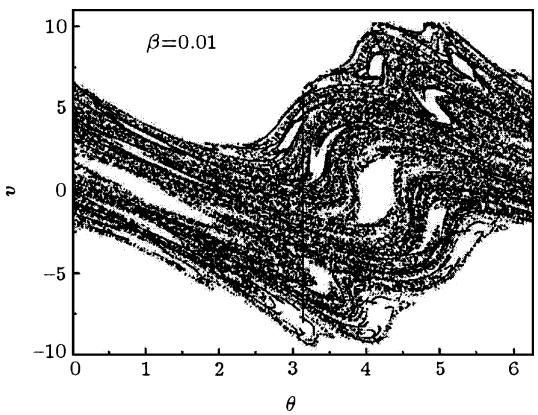


Fig.3. The transient stochastic web at $K = 4.65$, $\alpha = 1$, $v_0 = 5$ and β=0.01.

Figure 4 is drawn by evenly selecting 1000 initial points in the discontinuous borderline $\{(\theta, v)|_{\theta=\pi, v\in[-1,1]}\}$, ignoring the first 500000 iterations, and then recording the next 400 ones as $\beta = 0.01$. The figure will be exactly the same if we evenly select 1000 initial points in the range $\theta \in [0, 2\pi], v \in [-1, 1]$ instead. The results show that all the iterations in the stochastic web formed by the image set of the discontinuous borderline escape to some elliptic islands.

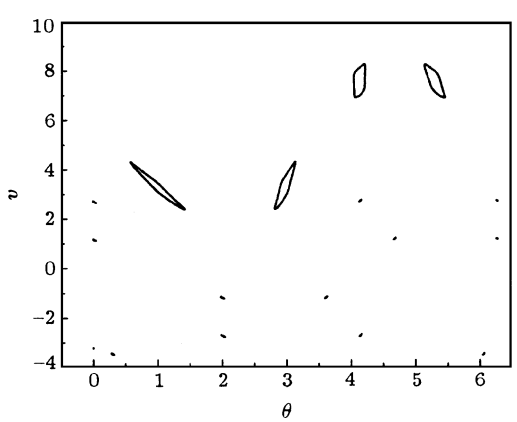


Fig.4. The attractors at $K = 4.65$, $\alpha = 1$, $v_0 = 5$ and β=0.01.

The sudden change of the conservative stochastic web to a transient one can be considered as a crisis.[20] There should be some "escaping channels" or "escaping holes", which connect the transient stochastic web and the islands so that the iterations in the web can escape to the islands through them. Since the dissipation in the current system comes from the appearance of two backward images of some phase points, it is reasonable to predict that the escaping holes should be the set of the points in the elliptic islands, which have two backward images. One of them is inside the islands and corresponds to a conservative motion; another is outside them and corresponds to a dissipative motion. It is not difficult to deduce the condition, under which a phase point, (v_{n+1}, θ_{n+1}), can have backward image.

$$\begin{aligned} &\pi - 2\mathrm{arctg}(v_{n+1}/v_0) \leq \theta_{n+1} \leq 2\pi \\ &-2\mathrm{arctg}(v_{n+1}/v_0) \quad \theta_n \in [0, \pi]\,, \end{aligned} \tag{5}$$

$$\begin{aligned} &2\pi - 2\mathrm{arctg}(v_{n+1}/(v_0 - \beta)) < \theta_{n+1} < 3\pi \\ &-2\mathrm{arctg}(v_{n+1}/(v_0 - \beta)) \quad \theta_n \in (\pi, 2\pi)\,. \end{aligned} \tag{6}$$

The conclusion is that (v_{n+1}, θ_{n+1}) have two backward images when Eqs.(5) and (6) are satisfied simultaneously. The two black curves in Fig.5 show the point set satisfying this condition when $K = 4.65$, $\alpha = 1$, $v_0 = 5$ and $\beta = 0.01$. The figure shows also that one of the curves intersects with the edge of one of the four elliptic islands, which belongs to the period-4 island chain mentioned in the last section. This result shows the escaping hole with the chosen parameters and also why only the edge parts of the island chain are shown in Fig.4 when we record the iterations after ignoring transients to show the attractors.

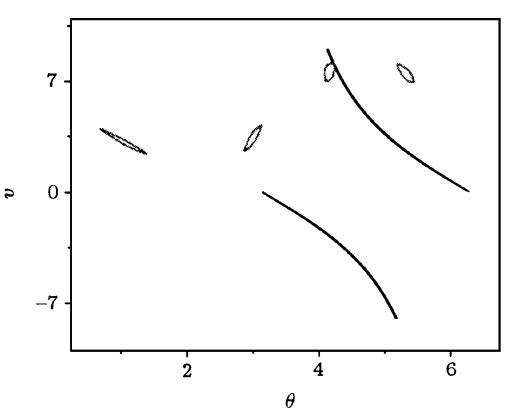


Fig.5. The period-4 elliptic island chain and the set satisfying Eqs.(5) and (6) at $K = 4.65$, $\alpha = 1$, $v_0 = 5$ and β=0.01.

Based on this understanding we can calculate and then determine the linear dependence of the area of

the escaping hole, Δ, on the control parameter, β, as shown in Fig.6.

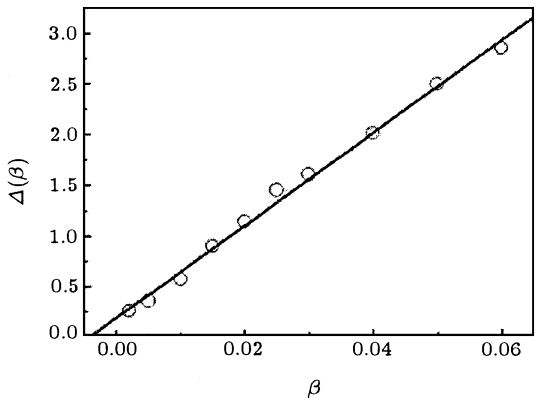


Fig.6. The linear dependence of the area of the escaping hole, Δ, on the control parameter, β.

To signify the gradual escape change from the transient stochastic web, an average lifetime, τ, is defined as

$$\langle\tau\rangle = \lim_{n\to\infty} \frac{\sum_{i=1}^{n} \tau_i}{n},$$

where n denotes the number of initial values and τ_i denotes the number of iterations in the transient stochastic web starting from the initial value i. Now, following Grebogi *et al*,[20] the special phase space contraction rate (in quasi-dissipative systems) influence on the lifetime scaling behaviour is considered. If the escaping hole takes an area Δ at a control parameter value β, the hole is iterated backwards in time for n steps and gives a region with an area Δ'. In an everywhere smooth and conventionally dissipative two-dimensional map, discussed in Ref.[20], the measure Δ depends on the unstable periodic orbit properties. However, in a quasi-dissipative two-dimensional map, it can simply be predicted that $\Delta' = 2m\Delta$, where $m < n$, since it is only in some iterations that two phase space pieces can iterate to one, and the much stronger exponential contraction (which appears in a conventionally dissipative system) is absent. Since the area of the leaking hole, Δ, is proportional to the control parameter value, β, and the probability, $P(\Delta)$, with which the iterations visit the hole, obeys a rule $P(\Delta) \propto \rho\Delta$, where ρ denotes the visiting probability to a unit area in Δ, for the iteration process from Δ' to Δ, one can obtain

$$\frac{P(\Delta)}{P(\Delta')} = \frac{\rho\Delta}{\rho\Delta'} = \frac{\beta}{2m\beta} = \frac{1}{2m}.$$

So, considering the widely accepted assumption $\langle\tau\rangle \propto \frac{1}{P(\Delta)}$, one has

$$\frac{\langle\tau\rangle_{\Delta}}{\langle\tau\rangle_{\Delta'}} = \frac{\langle\tau\rangle_{(\beta)}}{\langle\tau\rangle_{(2m\beta)}} = \frac{\beta^{-\gamma}}{(2m\beta)^{-\gamma}} = \frac{1}{(2m)^{-\gamma}} = \frac{P(\Delta')}{P(\Delta)} = \frac{1}{(2m)^{-1}}.$$

This means that this crisis has a special scaling exponent, $\gamma = 1$ in the power law $< \tau > \propto \beta^{-\gamma}$.

Figure 7 shows numerical results about the relationship between $< \tau >$ and the driving parameter β. The solid linear line on the double logarithmic plane shows the least square fitting of the data, which crosses four magnitude degrees and shows a good agreement with the power scaling law. The scaling exponent, $\gamma = 0.992 \pm 0.018$, agrees very well with the analytic discussion.

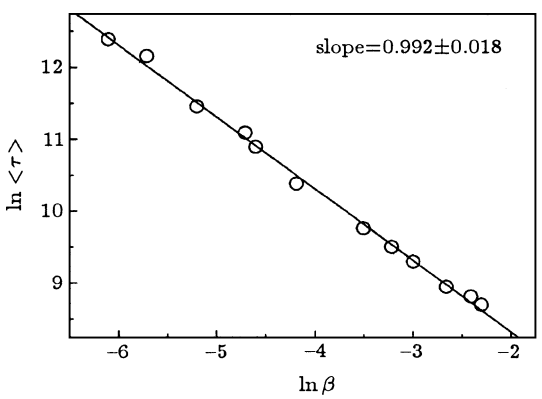


Fig.7. The power-law dependence of the averaged lifetime, $< \tau >$, on the control parameter, β.

4. Forbidden web

A forbidden region appears when the present system becomes piecewise continuous. To show this, we define the forbidden region of map (1), J_1, as the region where every point's backward image falls in the definition range of map (2), i.e. $f_1^{-1}(P) \in D_2$, and thus it does not exist. Similarly, we define the forbidden region of map (2), J_2, as the region where every point's backward image falls in the definition range of map (1), i.e. $f_2^{-1}(P) \in D_1$, and thus it does not exist also. Their expressions are:

$$J_1 : \pi \le \theta_{n+1} - \pi + 2\mathrm{arctg}\left(\frac{v_{n+1}}{v_0}\right) \le 2\pi, \quad (7)$$

$$J_2 : 0 < \theta_{n+1} - \pi + 2\mathrm{arctg}\left(\frac{v_{n+1}}{v_0 - \beta}\right) \le \pi. \quad (8)$$

The forbidden region of the system, where the iterations starting from any other places in the phase

plane cannot enter, is defined as $J = J_1 \cap J_2$. In Fig.8 J_1 is shown by a regions filling light black lines, J_2 is shown by a regions filling dark black lines; and the forbidden region, $J = J_1 \cap J_2$, is indicated by arrowheads and black regions. Comparing Eqs.(7), (8) with Eqs.(5), (6), one can see that the remnant two void regions are the places where (v_{n+1}, θ_{n+1}) has the two backward images that are shown in Fig.5.

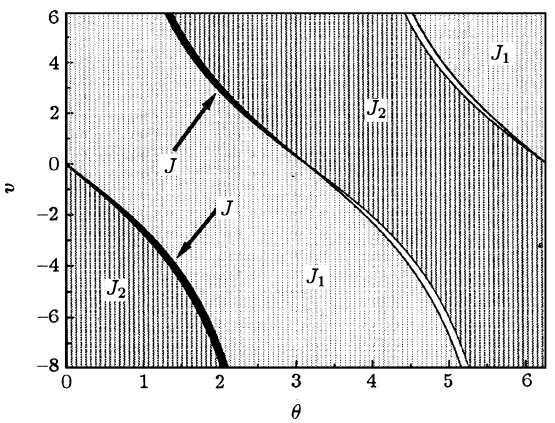


Fig.8. The forbidden region J_1, J_2 and J.

The forward images of J seem to be a forbidden region also, however some points there may have two backward images. One of them belongs to the forbidden region; the other is outside of it. Therefore the real forbidden region should be the forward image set of J excluding the points which have two backward images. This can be expressed as $\mathrm{Fr} = \bigcup_{j=1}^{\infty} [f^j(J) \backslash Q]$, where Q denotes the set of points which have two backward images. Obviously, Fr should be a fat fractal web. As shown in Fig.8, the boundaries of J are backward images of the discontinuous borderline produced by different submaps. For this reason the boundaries of the forbidden web, Fr, should be the forward images of the discontinuous borderline. That means the transient stochastic web and the forbidden web must be complementary in the phase space, as shown in Figs.9(a) and 9(b). In order to show this more clearly, we magnify the regions denoted by the rectangular in Fig.9(a) or 9(b) by Fig.9(c) or 9(d) so that one can see more detail, and choose the parameter value $\beta = 0.45$ instead of $\beta = 0.01$ so that the forbidden web becomes bigger.

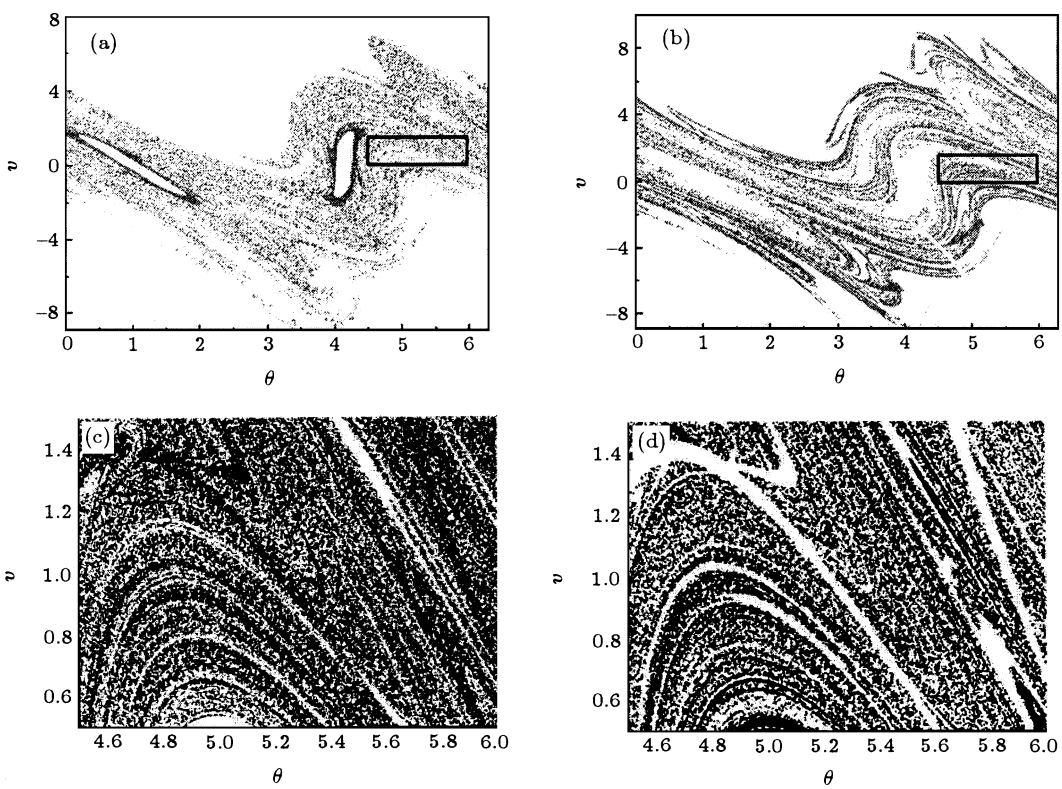


Fig.9. The stochastic (a) and the forbidden (b) webs at $\beta = 0.45$. The indicated regions in (a) and (b) are magnified and shown in (c) and (d) respectively.

Then the whole picture for the system evolution is as follows. A forbidden web formed mainly by the image set of the forbidden region J suddenly appears inside the original conservative stochastic web when the controlling parameter β becomes nonzero. The remnant is the transient stochastic web formed by the image set of the discontinuous borderlines. When β further progresses, the forbidden web grows so that the transient stochastic web becomes increasingly thinner. That makes the iterations in the transient stochastic web escape to the elliptic islands faster. Therefore, in addition to the lifetime scaling law of the iterations on the transient stochastic web, the crisis may be described by another rule, which expresses the change of the fat fractal forbidden web. This may be more important for the current sample of crisis.

The Hausdorff dimension of a fat fractal, which has a finite Lebesgue measure and a fractal shape, equals the dimension of the phase space where it is embedded. Therefore, the Hausdorff dimension is not a good quantity to describe the fat fractal set. One has to introduce a new quantity, which is suitable for both the thin and fat fractal. This is called the "fractal exponent" and is defined as[21−23]

$$\sigma = \lim_{\xi \to 0} \frac{\ln |\mu(A_\xi) - \mu_0|}{\ln \xi}, \tag{9}$$

where ξ denotes the scale, A_ξ represents the coarse set of the fat fractal under ξ (this means the remnant after wiping off all the holes larger than ξ), $\mu(A_\xi)$ represents the measure of A_ξ, and μ_0 the limit of $\mu(A_\xi)$ when $\xi \to 0$, i.e. $\mu_0 = \lim_{\xi \to 0} \mu(A_\xi)$. By using this method, we have calculated the fractal exponents of the forbidden web at some parameter values. As an example, Fig.10 shows the scaling-free region on the $\ln[\mu(A_\xi) - \mu_0] \sim \ln \xi$ plane when $\beta = 0.02$. The fractal exponent should equal the slope of the least square fitting line, which is $\sigma = 0.393 \pm 0.004$. Figure 11 shows the relationship between the so-calculated fractal exponents and the controlling parameter. The results show a perfect power law, $\sigma \propto \beta^\delta$, with a scaling exponent $\delta = 0.288 \pm 0.007$.

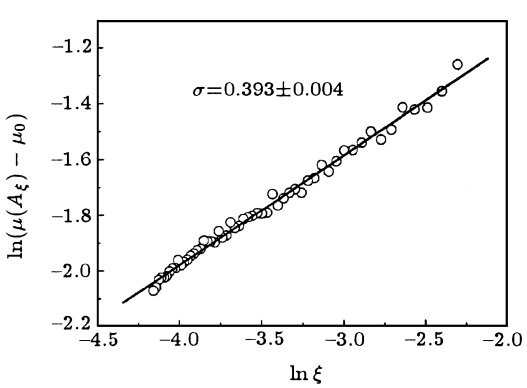


Fig.10. The scaling-free region on the $\ln[\mu(A_\xi) - \mu_0] \sim \ln \xi$ plane when $\beta = 0.02$.

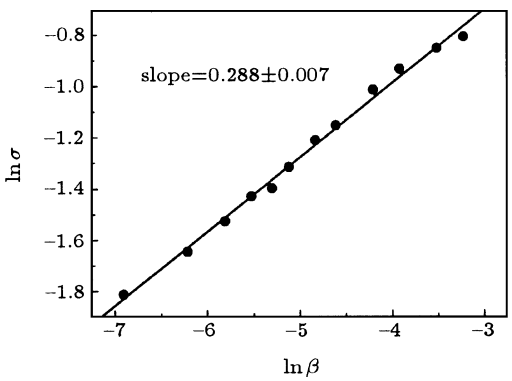


Fig.11. The relationship between the fractal exponents and the controlling parameter.

5. Conclusion and discussion

The crisis reported in this article has two characteristics. The first one is that although it obeys the universal lifetime power law, the scaling exponent takes a special value, 1. This is due to the linear contraction rate of the phase space in a quasi-dissipative system. The second one is the appearance of the fat-fractal-forbidden web. The remnant in the original conservative stochastic web after losing this forbidden web is the transient stochastic web formed by the image set of discontinuous borderlines. The iterations on this transient web escape to some elliptic islands. In addition to the ordinary lifetime power-law dependence, another power law, which describes the relationship between fractal exponents of the forbidden web and the controlling parameter may be more important for characterizing this crisis.

We believe that this kind of crisis exists in many quasi-dissipative systems. As an evidence, a very similar crisis has been observed in the electronic relaxation oscillator studied by Wang *et al.*[11] The results will be presented elsewhere.

References

[1] Zhusubaliyev Z T and Mosekide E 2003 *Bifurcation and Chaos in Piecewise-Smooth Dynamical Systems* (Singapore: World Scientific)

[2] Chua L O and Lin T 1988 *IEEE Trans. Circuits. Syst.* **35** 648

[3] Stikvoort E F 1988 *IEEE Trans. Commum.* **36** 1157

[4] Tsypkin Y Z 1984 *Relay Control Systems* (Cambridge: Cambridge University Press)

[5] Andronov A A, Khaikin S E and Vitt A A 1965 *Theory of Oscillations* (Oxford: Pergamon Press)

[6] Flugge-Lotz I 1968 *Discontinuous and Optimal Control* (New York: McGraw-Hill)

[7] Wiercigroch M and de Kraker B 2002 *Applied Nonlinear Dynamics and Chaos of Mechanical Systems with Discontinuities* (Singapore: World Scientific)

[8] Awrejcewicz J and Lamarque C H 2003 *Bifurcation and Chaos in Nonsmooth Mechanical Systems* (Singapore: World Scientific)

[9] Whiston G S 1985 *J. Sound Vib.* **188** 395; 1992 *J. Sound Vib.* **152** 427

[10] Chin W, Ott E, Nusse H E and Grebogi C 1994 *Phys. Rev.* E **50** 4427

[11] Wang J, Ding X L, Hu B, Wang B H, Mao J S and He D R 2001 *Phys. Rev.* E **64** 026202

[12] Wang J, Ding X L, Wang B H and He D R 2001 *Chin. Phys. Lett.* **18** 13

[13] Wang X M, Wang Y M, He D R *et al* 2002 *Eur. Phys. J.* D **19** 119

[14] Jiang Y M, Lu Y Q, He D R *et al* 2004 *Eur. Phys. J.* D **29** 285

[15] Ulam S 1961 in *Proc. 4th Berkeley Symposium on Mathematical Statistics and Probability* (Berkeley: University of California Press) Vol.3 p315

[16] Szymanski K and Labaye Y 1999 *Phys. Rev.* E **59** 2863

[17] Tureci H E, Schwefel H G L, Stone A D and Narimanov E E 2002 *A Gaussian-optical Approach to Stable Periodic Orbit Resonance of Partially Chaotic Dielectric Microcavities* arXiv:physics/0207003

[18] Reichl L E 1992 *The Transition to Chaos in Conservative Classical Systems: Quantum Manifestations* (New York: Springer) 1st edn.

[19] Mira C 1996 *Int. J. Bifurc. Chaos* **6** 893

[20] Grebogi C, Ott E and Yorke J A 1982 *Phys. Rev. Lett.* **48** 1507
Grebogi C, Ott E and Yorke J A 1983 *Physica* D **7** 181

[21] Grebogi C, McDonald S W, Ott E and Yorke J A 1985 *Phys. Lett.* A **110** 1

[22] Umberger D K and Farmer J D 1985 *Phys. Rev. Lett.* **55** 661

[23] Farmer J D 1986 in *Dimensions and Entropies in Chaotic Systems* ed. E. Mayer-Kress (Berlin: Springer) p54